Journal of Structural Engineering & Applied Mechanics
2021 Volume 4 Issue 3 Pages 140-150
https://doi.org/10.31462/jseam.2021.03140150

www.goldenlightpublish.com

RESEARCH ARTICLE

Seismic performance evaluation of a precast concrete structure with deformation-based limit criterions

Sadık Can Girgin[*1], Cem Göksoy[2], Emine Daş[2], İbrahim Serkan Mısır[1]

[1] *Dokuz Eylul University, Department of Civil Engineering, Izmir, Turkey*
[2] *Dokuz Eylul University, Graduate School of Natural and Applied Sciences, Izmir, Turkey*

Abstract

In precast reinforced concrete buildings, which constitute an important part of the industrial buildings in Turkey, the force flow between the structural elements is provided by beam-column connections with or without transferring moments. In general, moment resisting beam-column connections with mechanical or emulative components are applied at the mezzanine level. For precast concrete structures, strength-based design is the most common design approach in engineering practice. In recent years, performance based seismic design and evaluation approach also gained attention which provides numerical estimation of the damage in structural elements subjected to earthquake loading. This study presents the performance based seismic assessment of a two-story precast building based on the seismic evaluation requirements of Turkish Building Earthquake Code 2018. For this purpose, numerical simulation model has been established by using lumped plasticity models for connections and distributed plasticity models for columns. Strong ground motion records are scaled based on TBEC-2018 acceleration spectrum for a specific location, and nonlinear time history analyses are performed in *x* and *y* directions simultaneously. The performance evaluation results using average deformations show that there is a significant difference between plastic rotation and reinforcing bar strain performance limits.

Keywords

Precast concrete; Seismic performance; Deformation; Performance limit; Plastic rotation

Received: 12 June 2021; Accepted: 14 August 2021
ISSN: 2630-5763 (online)

1. Introduction

Reinforced concrete structures constitute a large portion of the existing building stock in Turkey, and vast number of these buildings that survived earthquakes with severe damage show brittle damage modes [1]. Most of the industrial buildings in Turkey are constructed as precast reinforced concrete systems, those are single-storey or partially intermediate-storey, large span, column systems built from foundation level (Type-1). In other part of precast industrial buildings, the force flow between the structural elements is ensured by beam-column connections those are hinged at the roof level and moment resisting connections at the floor level (Type-2). It was reported after the major earthquakes that the effects of beam-column connections in these precast concrete buildings have a significant impact on the overall building seismic performance [2, 3].

The design principles for strength and deformation-based approaches of prefabricated reinforced concrete buildings are stipulated within

* Corresponding author
Email: sadik.girgin@deu.edu.tr

the Turkish Earthquake Building Code-2018 (TBEC-2018) [4], thanks to recent experimental studies conducted to determine the cyclic behavior of these connections. Performance limits for structural members are provided in terms of material strains, also in terms of chord rotations in TBEC-2018 (also in ASCE/SEI 41, 2006) [5]. Hybrid (emulative welded) connections are commonly used moment-resisting connections in precast construction practice called as MAB3 in TBEC-2018. Hybrid connections are constructed by welding longitudinal rebars to plates embedded to precast beams and casting concrete through the formed gaps in beam and column elements at site. Damage pattern and lateral cyclic response of a precast beam-column connection is shown in Fig. 1 [6].

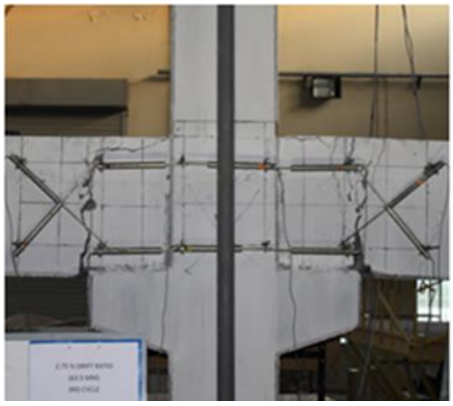

(a)

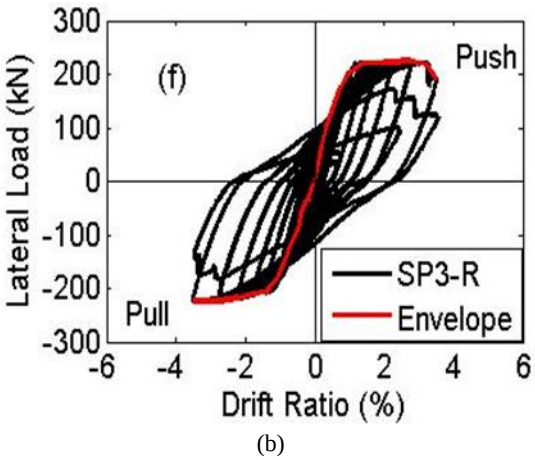

(b)

Fig. 1. (a) Damage pattern at 2.75 % drift ratio, and (b) Lateral load- drift ratio response for SP3-R specimen [6]

Performance-based seismic evaluation of structures has gained attention for two decades to estimate the seismic risk in a realistic manner. Magliulo et al. [7] performed nonlinear static and dynamic analyses on existing precast concrete structures considering all seismic components. They concluded that building failures due to beam damages and loss of support were caused by the variation of axial load near corner columns. Kayhan and Şenel [8] generated typical building models for precast concrete structures using a large structural database and performed nonlinear time history analyses with various structural parameters. It was reported that column dimensions and stirrup spacing had significant effect on the overall performance. Seismic behavior of one-storey industrial buildings with hinged connections at the roof level with and without dowels was studied by Deyanova et al. [9]. It was reported that the major factor affecting the global response was relative strength between column and connection. Casotto et al. [10] studied an analytical methodology accounting for variability of different parameters to classify industrial buildings in Italy. They performed damage scenario analysis on precast building models and obtained damage states for the building stock.

This study presents a numerical investigation on seismic response of an existing two storey precast building. For this purpose, a nonlinear 3D model was developed by assigning rotational springs at beam ends representing the moment-resisting beam-column connections. Besides, column sections were modeled by using fiber-based modeling approach in a plastic hinge zone. Nonlinear time history analyses were performed using earthquake records compatible with TBEC-2018 [4] spectra. Seismic performance of the existing structure was evaluated by deformation-based performance limit criterions based on section rotations, also using material strains.

2. Existing precast concrete structure

Existing two-storey precast building is with a plan size of 17×45 m, with an intermediate floor at +3.52 m elevation extending to all plan area along all the

openings, with a total height of 6.62 m. Element ends at roof level are hinged type, and at mezzanine level beam-column connections are designed to transfer moments with emulative-welded (MAB-3) connections. The façade columns of the building continue along two floors and the interior columns are only at the height of the intermediate floors. The building was designed as a school building on ZD ground class, in a location of high seismic risk considering controlled damage level using force-based design principles in TBEC (2018). Horizontal elastic acceleration spectrum characteristic values were determined as S_s = 1.15, S_1 = 0.288, F_s = 1.039 and F_1 = 2.024, based on the current Turkey Earthquake Hazard Map (TEHM) [11] by taking the Ground Motion Level DD2, and SDS = 1.198 and SD1 = 0.583. The precast concrete frame system in the direction of short span is shown in Fig. 2. C30 concrete and B420C reinforcing steel classes were taken into consideration for all structural elements. Cross sections and geometric details of the beam and column precast concrete elements and moment-resisting connections are shown in Fig. 3 [12].

The three-dimensional SAP2000 [13] model of the structure is given in Fig. 4. Diaphragm effect provided by roof covering material was modeled using equivalent truss method [14]. It has been assumed that the mezzanine floors at the elevation of +3.52 m will exhibit rigid diaphragm behavior. The first periods of the structure calculated for the short and long span directions, accounting for the cracked section stiffnesses of the elements are calculated as 0.54 s and 0.51 s, respectively (Fig. 4b). Roof truss elements are considered as pin-hinged connection (MFB1) with equivalent rectangular cross-sections. The structural system was analyzed using the Equivalent Earthquake Load Method under vertical and horizontal loads [12], and the frame element reinforcements were determined according to the most unfavorable combination specified in TBEC-2018 [4].

3. Nonlinear modeling of the structure

3.1. Numerical simulation model

It is assumed that the elements with hinged connections at the roof level behave linearly elastic. Within the scope of the study, lumped plasticity model was assigned to simulate the cyclic behavior of the emulative-welded beam-column connections (MAB3) located in the intermediate floor [12].

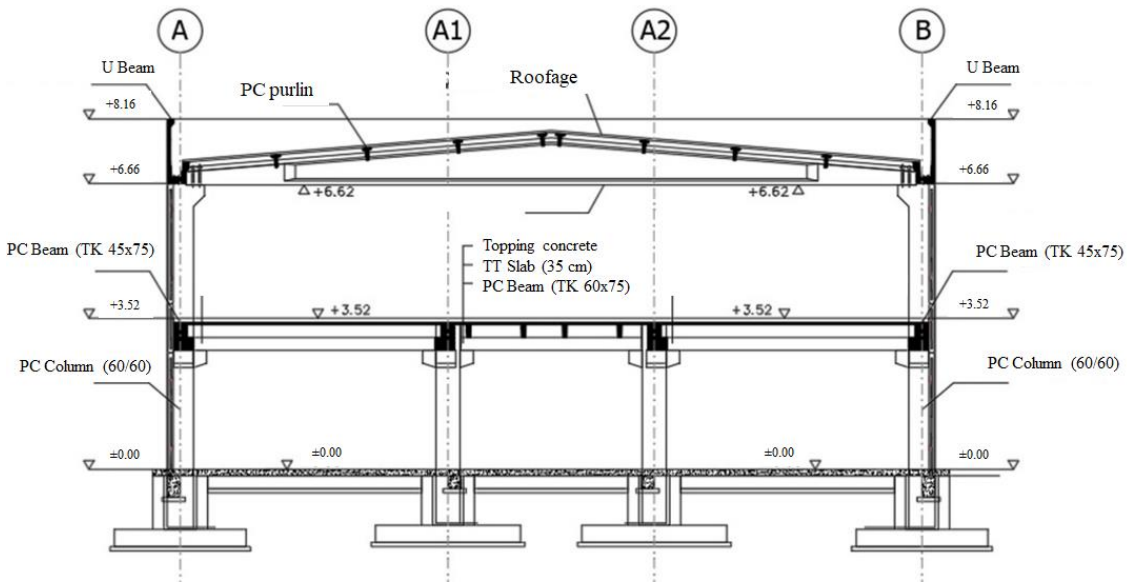

Fig. 2. Precast structural system in the short span direction [12]

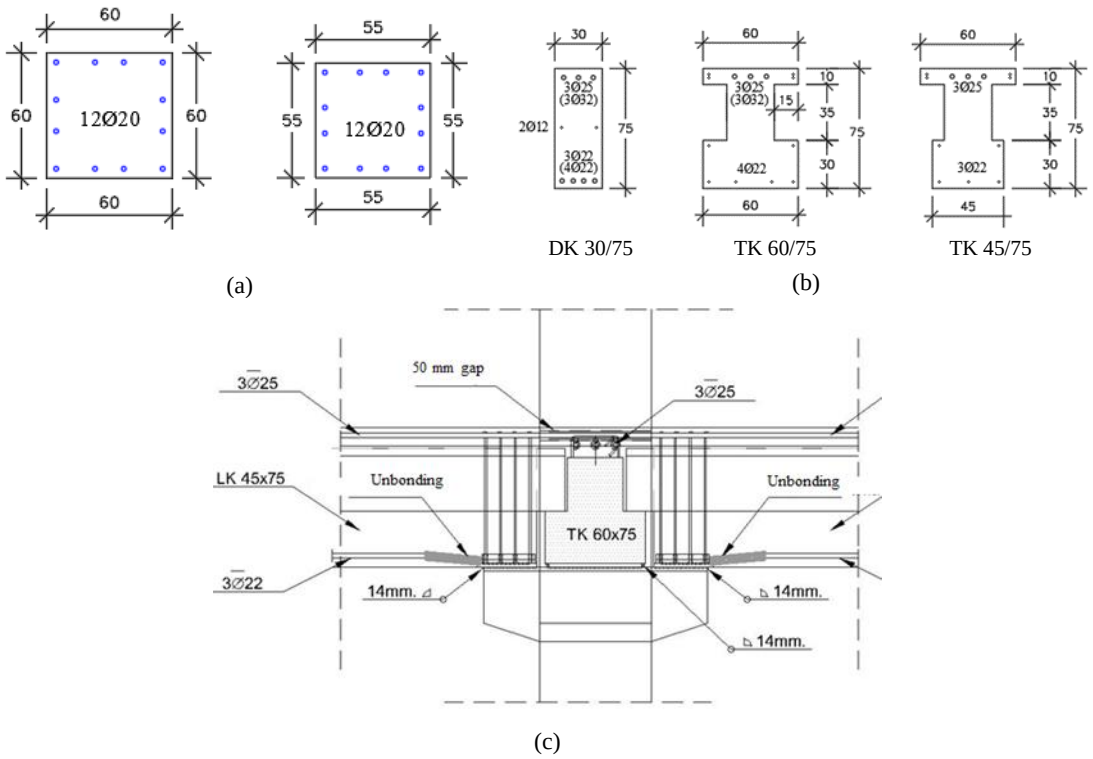

Fig. 3. a) Precast concrete column, b) Precast concrete beam geometric and reinforcing details, c) detail of the designed MAB3 type moment transfer connection [12]

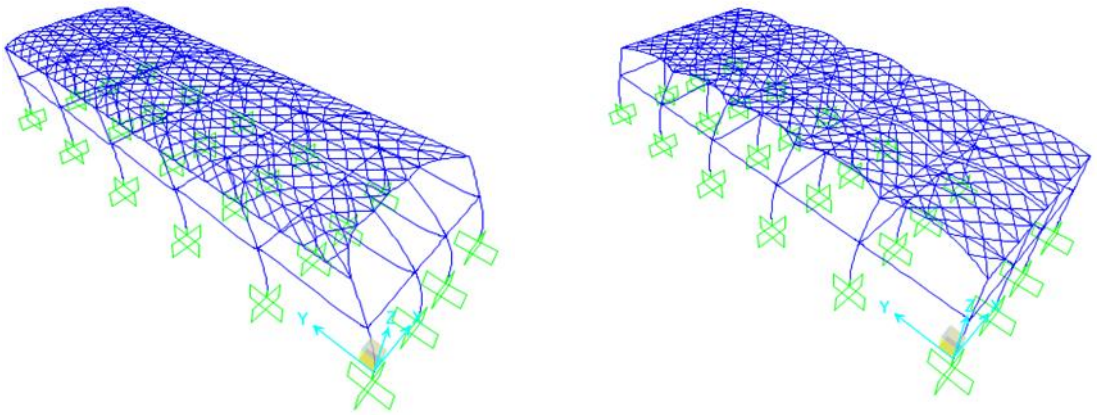

Fig.4. Mode shapes of the precast concrete structure (a) first mode shape (T_1=0.54 sec) and (b) second mode shape (T_2=0.51 sec)

The nonlinear behavior of the connections was represented with stiffness and strength degrading peak-oriented hysteretic response at beam ends as shown in Fig. 5a [15]. Modified Ibarra-Medina-Krawinkler (IMK) deterioration model [16] was adapted to Takeda model [17] to assign moment-resisting beam-column connections. Biskinis et al. [18] proposed an equation for the chord rotation at yield (θ_y) for beam-column elements with rectangular cross sections including flexure ($\theta_{flexure}$), shear (θ_{shear}) and bar slip (θ_{slip}) deformations as

$$\theta_y = \underbrace{\phi_y \frac{L_s + a_v z}{3}}_{\theta_{flexure}} + \underbrace{0.0013\left(1+1.5\frac{h}{L_s}\right)}_{\theta_{shear}} + \underbrace{a_{sl}\frac{0.13\phi_y d_b f_y}{\sqrt{f_c'}}}_{\theta_{slip}} \quad (1)$$

where ϕ_y is the yield curvature, L_s is the shear span, h is section depth, $[a_v z]$ is the tension shift due to diagonal cracking, z (= d – d') is the internal lever arm, a_v = 1 when there is diagonal cracking at flexural yielding, d_b is the diameter of tension reinforcement, a_{sl} is a coefficient for pull-out of rebars (a_{sl} = 1 if pull-out of longitudinal bars is occurred) and f_y and f_c' are the material yield and compressive strengths for steel and concrete, respectively.

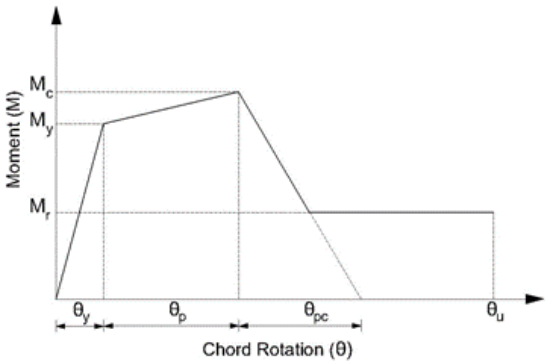

(a)

(b)

Fig. 5. (a) Lumped plasticity model for the beam-column connection [16], (b) Distributed plasticity model for columns [20]

Columns are modeled with fiber-based elements with fibers that each has uniaxial concrete or steel material properties in a plastic hinge length (L_p = 0.5h) in TBEC-2018 (Fig. 5b). Concrete material model based on Mander et al. [19] was assigned for unconfined and confined concrete sections. The stress-strain relation of cover concrete had unconfined concrete material model properties with compressive strength (f_c') occurring at ε_o (= 0.2%) strain. Compressive strength decreases to zero linearly at ε_u (= 0.5%) strain after the peak stress. For confined concrete of 60×60 cm column section, compressive strength (f_{cc}) =36.1 MPa, ε_{cc} = 0.0042, and ε_{cu} = 0.0113 were calculated. Reinforcing steel material was represented with bilinear material model parameters of force and deformation in SAP 2000 [13].

3.2. Selection and scaling of ground acceleration records

The procedure in TBEC-2018 [4] on the selection and scaling of earthquake records to be used in the definition of earthquake ground motions required for time history analyses are taken into consideration. According to TBEC-2018, the soil class was found to be ZD in the area where the existing building is located. The horizontal elastic design acceleration spectrum was constructed using the updated Turkey Earthquake Hazard Map (TEHM) [11], and the target spectrum was obtained by increasing the spectrum ordinates for the building importance factor 1.5. Unscaled ground motion data set proposed by Fahjan et al. [21] was obtained from the PEER database [22]. The information of the earthquake record sets evaluated within the scope of this study are given in Table 1. Real ground motion records differ in terms of maximum ground acceleration, frequency content, active times, etc. Therefore, they must be scaled to reflect a similar earthquake level. At this stage, seven sets of strong ground motion acceleration records were used, and the selected records were scaled to provide spectral compatibility by considering the target design spectrum in SeismoMatch software [23], which has been recognized for its competence in this field. The

average of the transformed earthquake ground motion spectra was greater than the design spectrum ordinates for all periods as required in TBEC-2018. In the scaling process, the geometric mean of the spectrum curves of the scaled ground motion records was checked with the mean and the largest mismatch value, and it was shown that it is provided for each direction. Earthquake records converted to spectral acceleration-period graph as shown in Fig. 6a on the design spectrum; The averages of the converted earthquake ground motion spectra are shown in Fig. 6b.

4. Seismic performance evaluation

Acceptable damage limits are defined to be compatible with the anticipated performance levels for different intensity levels of earthquakes in performance based seismic design and evaluation of existing structures. Performance levels for structural elements defined in TBEC-2018 are limited damage (LD)/immediate occupancy (IO), controlled damage (CD)/life safety (LS) and collapse prevention (CP). Seismic performance assessment of existing buildings in TBEC-2018 [4] is stipulated by means of elastic and inelastic analysis methods. Performance limit states for structural elements at different damage levels are defined as rotation-based or strain-based in ASCE/SEI 41 [5] and TBEC-2018 [4].

4.1. Evaluation of beam-column connections

In the draft version of TBEC [24], nonlinear analysis procedures were considered in deformation-based design of precast concrete structures. Performance limits for moment-resisting precast beam-column connections were determined according to ASCE/SEI 41 [5] considering experimental observations on MAB3 specimens tested by Girgin et al. [6].

Table 1. Selected and scaled strong ground motion records

Ground motion record	Year	Station	Record No	Mag	H1 Rec	H2 Rec
Imperial Valley-06	1979	El Centro Array #12	RSN175	6.53	H-E12140	H-E12230
Superstition Hills-02	1987	Westmorland Fire Sta	RSN728	6.54	B-WSM090	B-WSM180
Northridge-01	1994	El Monte - Fairview Av	RSN970	6.69	FAI095	FAI185
Landers	1992	Amboy	RSN832	7.28	ABY000	ABY090
Northridge-01	1994	LA - Pico & Sentous	RSN1000	6.69	PIC090	PIC180
Landers	1992	Baker Fire Station	RSN836	7.28	BAK050	BAK140
Imperial Valley-06	1979	Calipatria Fire Station	RSN163	6.53	H-CAL225	H-CAL315

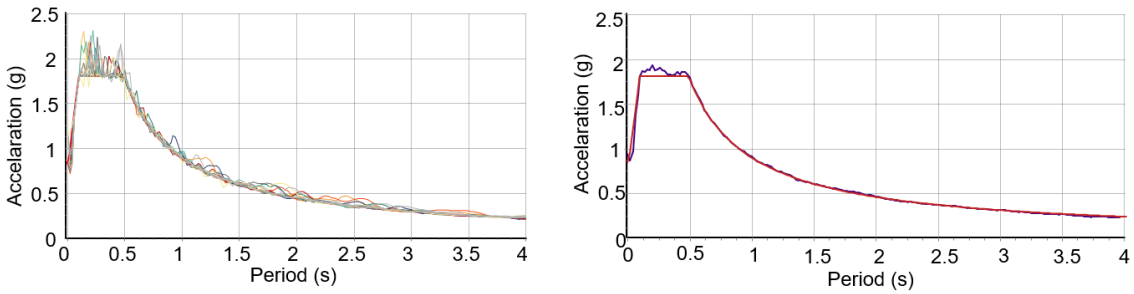

(a) (b)

Fig. 6. a) the spectra of the scaled strong ground acceleration records; and b) the average curve [12]

Performance limit states, and the corresponding drift ratios for precast connection tests are summarized in Table 2. The values in life safety (LS) performance level should be 0.75 times the deformation at point C which corresponds to collapse prevention (CP) performance level as given in ASCE/SEI 41 [5]. Therefore, obtained chord rotations (total rotation) for certain performance limits in Table 2 are consistent with the moment-chord rotations shown in Fig. 7 [24].

Fig. 8 presents the average plastic rotations gathered from analysis results of precast beam-column connections of the existing structure. Maximum plastic rotation was 0.023 rad of the moment resisting connections in the higher damage (H.D) zone. Fig. 9 shows the moment-rotation response of a moment-resisting beam-column connection in the higher damage zone.

Table 2. Performance limit states for precast composite connections

Performance Levels	Observed Damage States	Chord Rotation (rad)	Drift Ratio (%)
IO/ LD	Minor cracks at the connection	0.012	1.0
LS / CD	Spalling of concrete cover at the connection	0.025	2.2
CP	Significant shear cracks at the connection and buckling of beam bottom rebars	0.035	2.75

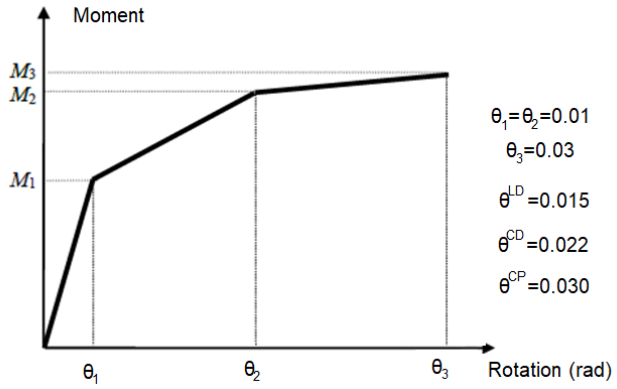

Fig. 7. Moment- rotation relationships for MAB 3 precast beam-column connections [24]

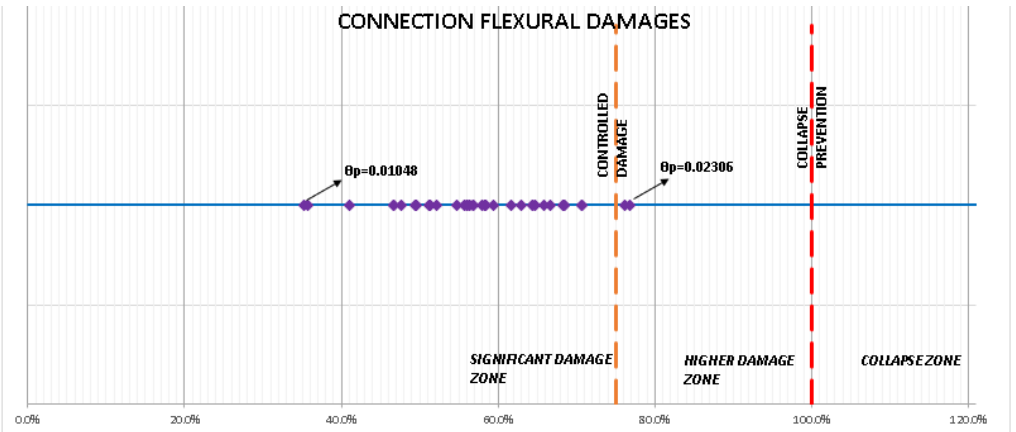

Fig. 8. Damage states of moment-resisting beam-column connections in terms of average plastic rotations

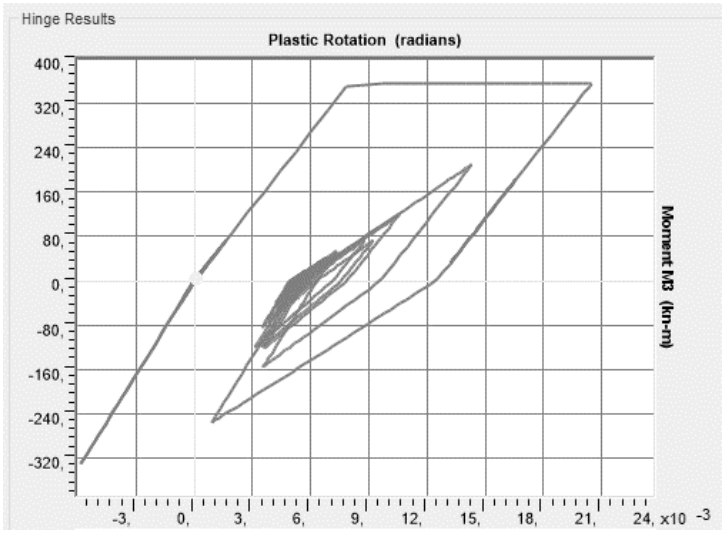

Fig. 9. Moment-rotation response of the beam-column connection

4.2. Evaluation of precast concrete columns

In TBEC-2018 [4], section deformation limits are defined in terms of plastic rotations and strains with the following equations as

$$\theta_P^{(CP)} = \frac{2}{3}\left[(\phi_u - \phi_y)\, L_P \left(1 - 0.5\frac{L_P}{L_S}\right) + 4.5\, \phi_u\, d_b\right] \quad (2)$$

$$\theta_P^{(CD)} = 0.75\, \theta_P^{(CP)} \quad (3)$$

$$\theta_P^{(LD)} = 0 \quad (4)$$

$$\varepsilon_c^{(CP)} = 0.0035 + 0.04\sqrt{\omega_{Ce}} \leq 0.018 \quad (5)$$

$$\varepsilon_s^{(CP)} = 0.4\varepsilon_{su} \quad (6)$$

$$\varepsilon_c^{(CD)} = 0.75\varepsilon_c^{(CP)} \quad (7)$$

$$\varepsilon_s^{(CD)} = 0.75\varepsilon_s^{(CP)} \quad (8)$$

where ϕ_u is ultimate curvature, ϕ_y is yield curvature, L_p is plastic hinge length (0.5h), L_s is shear span, ω_{ce} is effectiveness coefficient of confinement reinforcement, ε_{su} is ultimate strain of reinforcement. Precast columns in the existing structure were evaluated in terms of plastic rotations and strains and the results are presented below. Maximum attained plastic rotation is 0.029 rad of 2 columns in the higher damage zone (H.D.) as shown in Fig. 10. Fig. 11 shows the moment-rotation response of a moment-resisting beam-column connection in the collapse zone.

Precast columns are also evaluated according to strain performance limits of concrete and longitudinal reinforcing bars due to TBEC-2018 requirements. Fig. 12 shows the concrete core and rebar strain limits with corresponding number of columns in the damage zones. Performance evaluation according to concrete strain, the structure is at the higher damage zone and 4 columns exceed controlled damage (life safety) performance limit (Fig. 12a). On the other hand, longitudinal reinforcing bar strains in 12 precast columns reached beyond strain limit at collapse prevention $\varepsilon_s^{(CP)}$(=0.032) (Fig. 12b). These columns showed a significant difference in terms of damage levels for two types of evaluation criteria; plastic rotations and rebar strains as shown in Table 3. Concrete strain limits are compatible with plastic rotations of 10 columns which are in the collapse zone with 40% of all columns. Seismic performance of precast columns are presented in terms of number of columns within the defined damage zones due to plastic rotation and strain based criterions are summarized in Table 3.

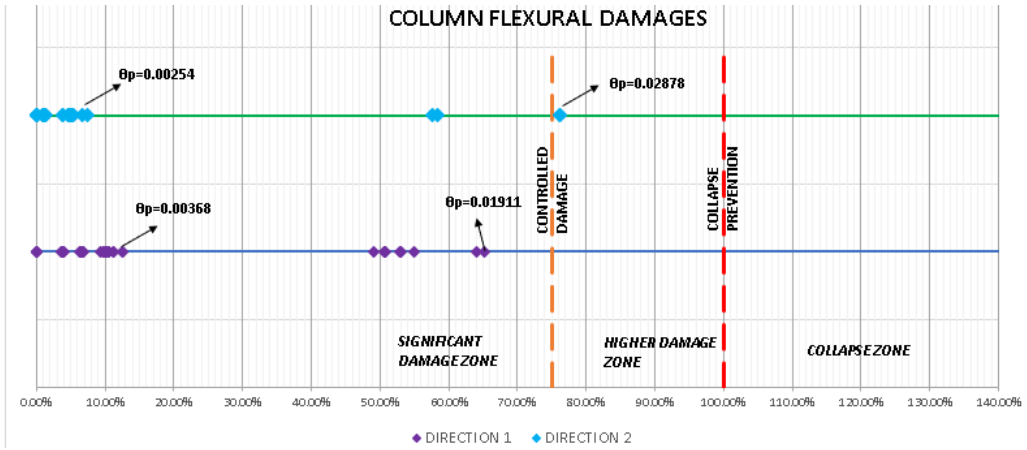

Fig. 10. Column damage states in terms of average plastic rotations

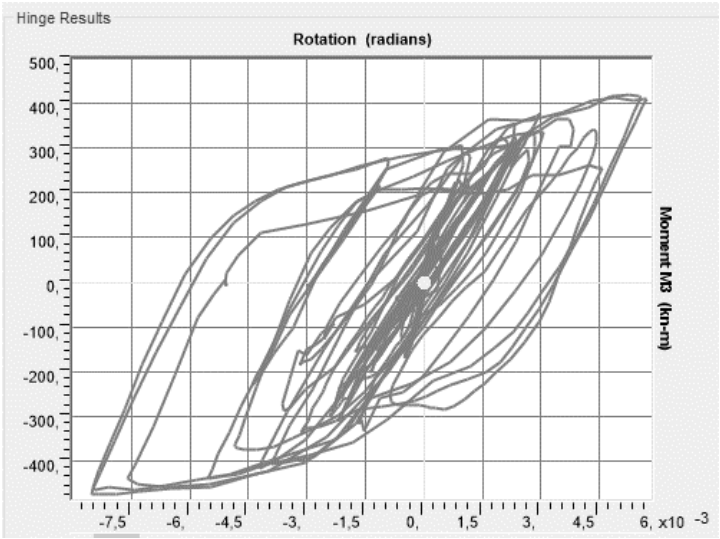

Fig. 11. Moment- rotation response of the precast concrete column

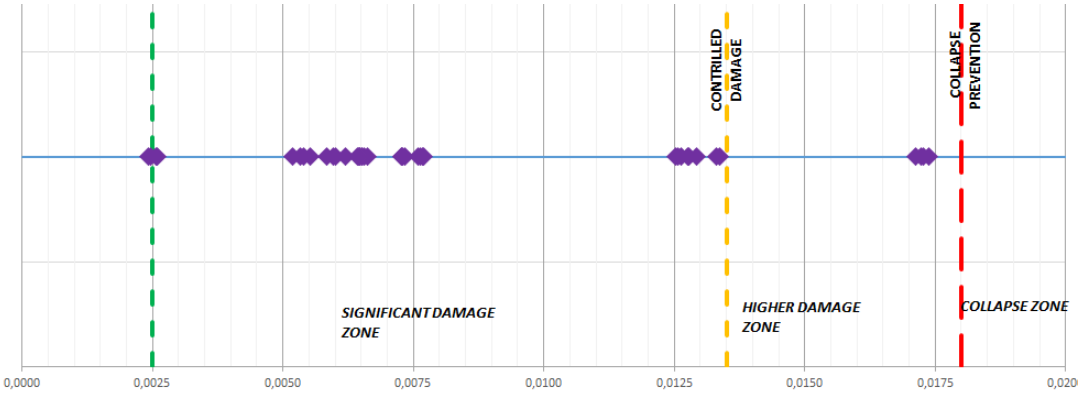

(a)

Fig. 12. Column damage states in terms of (a) core concrete strains, (b) reinforcing bar strains

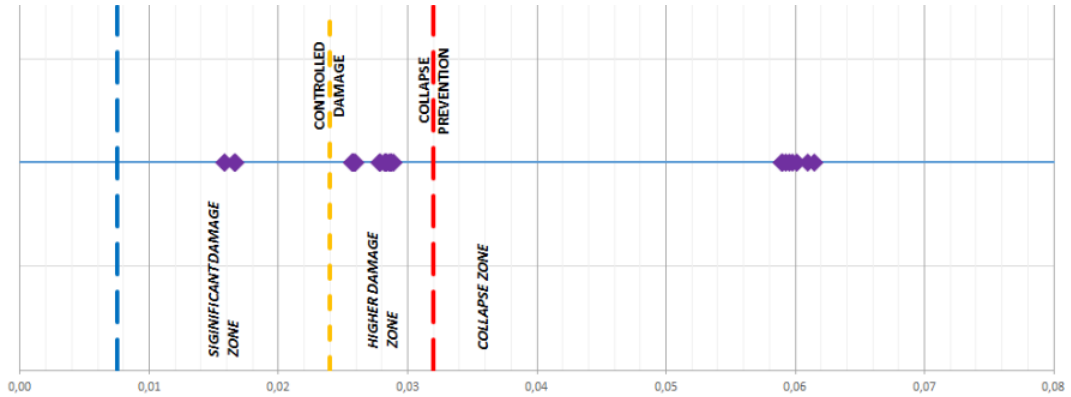

(b)

Fig. 12. Continued

Table 3. Seismic performance evaluation of precast concrete columns

Evaluation Parameter	L.D.	S.D.	H.D.	C.	Number of Columns Exceeding TBEC-2019	Number of Total Columns
Rotation	2	36	2	0	2	
Concrete Strain	0	36	4	0	4	40
Rebar Strain	0	1	27	12	39	

5. Conclusions

This study has presented numerical performance evaluation of a two-story existing precast concrete school building. Nonlinear time history analyses were performed under scaled earthquake records to obtain overall structural performance. Average response quantities such as plastic rotations and section strains were obtained and compared with the performance limits in TBEC-201). Since there is not an approach proposed in TBEC-2018 for performance based seismic evaluation of precast connections, beam-column connections were represented by a model based on experimental data and observations in the simulations. Beam-column connections remain in the controlled damage zone and 5% of the connections were in the collapse zone. Performance level of precast columns were within the significant damage zone with 90% in terms of computed average plastic rotations and concrete strains. However, using the seismic assessment in terms of rebar strains, performance levels of columns were 68% in higher damage zone and 30% in collapse zone. These results show that further studies should be performed to determine deformation-based performance limits in TBEC-2018 Code revisions accounting for the differences in terms of rotation and strains in precast concrete elements.

Declaration of conflicting interests

The author(s) declared no potential conflicts of interest with respect to the research, authorship, and/or publication of this article.

References

[1] Atmaca B, Demir S, Günaydın M, Altunışık AC, Hüsem M, Ateş Ş, Adanur S., Angın Z. (2020) Lessons learned from the past earthquakes on building performance in Turkey. J. Struct. Eng. Appl. Mech 3(2):61-84.

[2] Saatcioglu M, Mitchell D, Tinawi R, Gardner NJ, Gillies AG, Ghobarah A et al. (2001) The August 17, 1999 Kocaeli (Turkey) earthquake-damage to structures. Canadian Journal of Civil Engineering 28(4):715–737.

[3] Senel S, Palanci M (2013) Structural aspects and seismic performance of 1-story precast buildings in Turkey. Journal of Performance of Constructed Facilities 27(4):437-449.

[4] TBEC (2018) Turkish Earthquake Building Code. Disaster and Emergency Management Presidency, Ankara.

[5] ASCE SEI Committee 41 (2006) Seismic Rehabilitation of Existing Buildings, ASCE/SEI 41, Reston, VA, USA.

[6] Girgin SC, Misir IS, Kahraman S (2017) Experimental cyclic behavior of precast hybrid beam-column connections with welded components. International Journal of Concrete Structures and Materials 11(2):229-245.

[7] Magliulo G, Fabbrocino G, Manfredi G (2008) Seismic assessment of existing precast industrial buildings using static and dynamic nonlinear analyses. Engineering Structures 30(9):2580-2588.

[8] Kayhan AH, Şenel ŞM (2010) Fragility curves for single story precast industrial buildings. Teknik Dergi 21(104):5161-5184 (in Turkish).

[9] Deyanova M, Pampanin S, Nascimbene R (2014) Assessment of single-storey precast concrete industrial buildings with hinged beam-column connections with and without dowels. In Proceedings of the Second European Conference on Earthquake Engineering and Seismology, İstanbul.

[10] Casotto C, Silva V, Crowley H, Pinho R, Nascimbene R (2014) Scenario damage analysis of RC precast industrial structures in Tuscany, Italy. In Second European Conference on Earthquake Engineering and Seismology, Istanbul.

[11] TEHM (2018) Turkey Earthquake Hazard Maps Interactive Web Application. Disaster and Emergency Management Presidency. https://tdth.afad.gov.tr/TDTH/

[12] Mısır İS, Girgin SC, Daş D, Göksoy C, Eraslan F, Demirbaş H, Koçbulut H (2019) Force and deformation-based design of precast reinforced concrete industrial buildings within the scope of Turkish Earthquake Code 2019. 5th International Conference on Earthquake Engineering and Seismology (in Turkish).

[13] Wilson EL, Habibullah A (2019) SAP 2000 Software, Version V20.2.0. Computer and Structures, Inc. (CSI), Berkeley.

[14] Yüksel E, Özkaynak H, Soydan C, Güllü A (2019) In-plane behavior of sandwich panels and their contribution to roof diaphragm stiffness, Precast Concrete Journal, Turkish Precast Concrete Association 129:5-13 (in Turkish).

[15] Girgin SC, Mısır İS, Kahraman S (2018) Experimental and numerical investigation of cyclic response of precast hybrid beam-column connections. In International Workshop on Advanced Materials and Innovative Systems in Structural Engineering: Seismic Practices.

[16] Ibarra LF, Medina RA, Krawinkler H (2005) Hysteretic models that incorporate strength and stiffness deterioration. Earthquake Engineering and Structural Dynamics 34(12):1489-1511.

[17] Takeda T, Sozen MA, Nielsen NN (1970) RC response to simulated earthquakes. Journal of Structural Division 96:2557- 2573.

[18] Biskinis DE, Roupakias GK, Fardis MN (2004) Degradation of shear strength of reinforced concrete members with inelastic cyclic displacements. ACI Structural Journal 101(6):773-783.

[19] Mander JB, Priestley MJN, Park R (1988) Theoretical stress-strain model form confined concrete. Journal of Structural Division 114(8):1804-1826.

[20] Engineering Laboratory of the National Institute of Standards and Technology (NIST) (2013) Nonlinear Analysis Research and Development Program for Performance-Based Seismic Engineering. Technical Report. Grant No: NIST GCR 14-917-27.

[21] Fahjan YM (2008) Selection and scaling of real earthquake accelerograms to fit the Turkish design spectra. Teknik Dergi (Digest) December:1231-1250.

[22] Pacific Earthquake Engineering Research Center (PEER) (2014) PEER NGA Ground Motion Database. https://ngawest2.berkeley.edu/site [Accessed July 2019].

[23] SeismoSoft (2018) SeismoMatch: A computer application capable of adjusting earthquake accelerograms to match a specific target response spectrum, Version 2018.

[24] TBEC (2016) Turkish Earthquake Building Code (Draft Version). Disaster and Emergency Management Presidency, Ankara.